Presented at ION GNSS+ 2014, Session E6a, Tampa, Florida, USA, September 8-12, 2014.

An Efficient Time-Frequency Algorithm for Weak Signal Acquisition of Modernized GNSS Signals

Yanguang Wang, Jia Tian, Jérôme Leclère, Cyril Botteron, Vincenzo Capuano, Pierre-André Farine
École Polytechnique Fédérale de Lausanne (EPFL),
Electronics and Signal Processing Laboratory (ESPLAB), Switzerland

BIOGRAPHY

Yanguang Wang received the Master Degree in Electronics and Signal Processing from the Xidian University, Xi'an, China, in 2007. He is currently working in the GNSS field at École Polytechnique Fédérale de Lausanne (EPFL), focusing his researches in the acquisition and high sensitivity areas, with application to hardware receivers.

Dr. Cyril Botteron is leading, managing, and coaching the research and project activities of the Global Navigation Satellite System and Ultra-Wideband and mm-wave groups at Ecole Polytechnique Fédérale de Lausanne (EPFL). He is the author or co-author of 5 patents and over 80 publications in major journals and conferences in the fields of wireless positioning systems, GNSS-based navigation and sensing, ultra-low-power radio frequency communications and integrated circuits design, and baseband analog and digital signal processing.

Prof. Pierre-André Farine is professor in electronics and signal processing at EPFL, and is head of the electronics and signal processing laboratory. He received the M.Sc. and Ph.D. degrees in Micro technology from the University of Neuchâtel, Switzerland, in 1978 and 1984, respectively. He is active in the study and implementation of low-power solutions for applications covering wireless telecommunications, ultra-wideband, global navigation satellite systems, and video and audio processing. He is the author or co-author of more than 100 publications in conference and technical journals and 50 patent families (more than 270 patents).

ABSTRACT

The new GPS/Galileo/Compass signals use much longer code lengths and higher code frequencies than the GPS L1 C/A signal. As a result, they can provide improved ranging and anti-jamming performances. Unfortunately, their acquisition complexity is significantly higher, especially in the high sensitivity or weak signal acquisition context. Acquisition of very weak signals requires long integration times, but the integration time is often limited because of the code phase shifting induced in the receiver by an unmatched code frequency. Therefore, for the purpose of minimizing the acquisition time, a new algorithm that we named "slope parallel frequency and code searching (SPFCS)", has been developed and is presented in this paper. This algorithm combines the parallel frequency searching and parallel code phase searching together in a novel way, and satisfies the requirements for providing standalone high sensitivity (i.e., without any network or additional sensors' assistance). In order to assess its performance, we consider in this paper the acquisition of the GPS L5 pilot signal. Our simulation results indicate that the proposed algorithm can successfully acquire, without assistance, L5 signals as low as 15 dB-Hz with 35 kHz Doppler shifts, and a computational burden over 2 to 4 times smaller at 15 dB-Hz and 18 dB-Hz, respectively, as compared to the traditional parallel code phase search (PCS) or double block zero padding (DBZP) methods.

1. INTRODUCTION

GNSS satellites modulate an L-band RF carrier by a pseudo random noise (PRN) code, which is in turn modulated by a navigation message or a secondary code. One of the most difficult tasks of a GNSS receiver is the acquisition of new satellite signals and in particular the synchronization process with code phase and carrier frequency. Under clear view of the sky (i.e., $C/N_0 \geq 45$dB-Hz), an integration of the local signal with the received signal over a single primary code is sufficient, and the initial synchronization process thus induces only a small computational burden and leads to a short processing time. However, in the high sensitivity context, the received power can be attenuated by over 30 dB. In this case, a significant extended signal processing gain (and thus integration time) is required to minimize the power of the background noise.

In order to minimize the acquisition time for both traditional (GPS L1 C/A signal) and modernized (e.g., GPS L5, Galileo E5 signals) signals, the parallel frequency search (PFS) or the PCS using a fast Fourier transform (FFT) are typically implemented [1, 2, 3]. If the traditional PFS algorithm is used for the acquisition of modernized GNSS signals such as GPS L5 and Galileo E5, the acquisition time might be prolonged significantly since their primary PRN codes are 10 times longer than the L1 C/A code. This acquisition time will also be prolonged significantly if the traditional PCS or DBZP algorithm is used, due to the increase in the number of frequency bins because of the 10 times higher code Doppler [4]. This problem will not be solved by the recently proposed DBZPTI algorithm [5] (where the last "TI" letters stands for transition insensitive) which provides an improvement over the DBZP method when bit transitions are present, but which performance also depends on the incoming Doppler frequency. Especially

in high sensitivity environments, the residual code Doppler will have a strong influence on the GNSS signal acquisition procedure and obviously will extend the acquisition time of the GNSS receiver. Therefore, some new methods are needed to minimize the acquisition time and computational burden.

In this paper, the problems mentioned above are solved by a new acquisition algorithm, which relies on the pilot channel of modernized GNSS signals. This algorithm is efficient both in terms of frequency estimation accuracy and computational burden.

The rest of the paper is organized as follows: Section 2 gives the model of the GNSS signals of interest. In Section 3, a short review of the fast acquisition algorithms of GNSS signals and of their drawbacks is given. In Section 4, the proposed SPFCS algorithm is detailed. In Section 5, an application example is discussed, focusing on the analysis of the computational burden. Section 6 presents the processing loss of the proposed algorithm. Section 7 shows the simulation results in different contexts. Finally, Section 8 summarizes the advantages of this algorithm.

2. SIGNAL MODEL

As the pilot channel of the GPS L5 signal and Galileo E5a or E5b has a similar signal structure, this study is applicable for all these signals and can be easily generalized to other signals as well. In the following, GPS L5 signal is taken as an example. The GPS L5 signal consists of two carrier components that are in phase quadrature with each other. Each carrier component is binary phase shift keying (BPSK) modulated by a separate bit train. One bit train is the modulo-2 sum of the I5-code, navigation data, and a secondary code, while the other is the modulo-2 sum of the Q5-code and a secondary code, with no navigation data. The latter is thus called the pilot channel. For a particular SV, all transmitted signal elements (carrier, codes, secondary codes, and data) are coherently derived from the same on-board frequency source [6]. The GPS L5 pilot signal emitted by a satellite i can be expressed as

$$s_i(t) = a\cos(2\pi f_L t)c_i(t)d_i(t), \quad (1)$$

where a is the amplitude of the signal, f_L is the carrier frequency (1176.45 MHz), c_i is the PRN code associated to the satellite which has a frequency of 10.23 MHz and a length of 10 230 chips, and d_i is the secondary code (NH20), which has a frequency of 1000 Hz and a length of 20 chips.

At the receiver side, the received RF signal which is the sum of several GNSS signals, is converted to an intermediate frequency (IF) through a front-end. After down-conversion and sampling, the signal at the input of the signal processing block can be expressed as [1]

$$s(n) = \sum_{i=1}^{L} \left\{ \begin{array}{l} a_i \exp\left[j\left(2\pi\left(f_{IF} + f_{D,i}\right)\right)nT_s + \theta_i \right] \\ \times c_i\left[\left(1+\frac{f_{D,i}}{f_L}\right)nT_s - \tau_i\right] d_i\left(nT_s - \tau_i\right) \end{array} \right\} + n_{i\,IF} + jn_{q\,IF}, \quad (2)$$

where n is an integer, L is the number of the received signals, T_s is the interval of two successive samples, f_{IF} is the intermediate frequency, $f_{D,i}$ is the Doppler frequency of the satellite i, θ_i is the carrier phase of the satellite i, τ_i is the code delay for the satellite i, and n_{iIF}, jn_{qIF} are independent white Gaussian noises with zero mean and a variance σ^2 coming from the thermal noise. The carrier-to-noise density of the sampled signal is $C/N_0=a^2/2\sigma^2T_s$ for a complex signal, and $C/N_0=a^2/4\sigma^2T_s$ for a real signal.

3. SIGNAL ACQUISITION

As discussed in [7], the purpose of the acquisition process is to determine the presence of a desired GNSS signal, and to estimate its precise code delay τ_i and Doppler shift $f_{D,i}$. To do so, the acquisition process correlates the incoming signal $s(n)$ with a replica signal to measure the similarity between the two signals. If the output of the correlator is larger than a threshold, the desired signal is assumed to be present; otherwise the desired signal is considered not present.

For the purpose of enhancing the performance of the acquisition process, FFT-based parallel searching methods have been widely developed and used. The PCS method is based on the circular correlation using FFT. Thanks to the relationship between the convolution in the time domain and the multiplication in the frequency domain, it is possible to compute the circular correlation of two signals s(n) and c(n) using the FFT and the Inverse FFT (IFFT) as

$$r_{sc}(n) = IFFT\left\{FFT\left[s(n)\right]FFT\left[c(n)\right]^*\right\}. \quad (3)$$

The corresponding architecture is illustrated in Figure 1, where the FFTs and the IFFT are typically performed on one period of the code. The IFFT results are then added to perform the coherent integration. The magnitude computation and the non-coherent integration are then performed. The lengths of the coherent N_c and non-coherent times N_{Nc} depend on the sensitivity and Doppler searching space requirements.

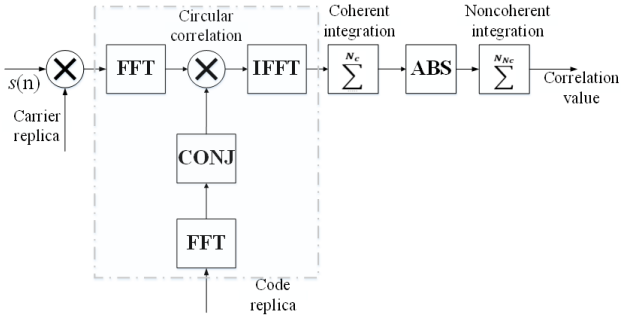

Figure 1 : Diagram of PCS algorithm

However, if the basic PCS approach is used for the GPS L5 signal acquisition in a high sensitivity context requiring long coherent integration times exceeding the primary code length, the unknown secondary code modulation would make it inefficient, due to potential transitions. But this problem can be solved by the DBZP approach [1, 8, 9], which can be seen as an enhanced PCS method. As depicted in Figure 2, in this method, the

length of the input of the FFTs is doubled, with two successive blocks of signal, and the counterpart of the local code FFT module is doubled with one period of the code and a vector of zeros. In this way, the original data vector ([$\boldsymbol{Block}_{signal}(1)$ $\boldsymbol{Block}_{signal}(2)$]) (Bold font means that it represent a vector) always contains an entire code period of the signal without any bit transition due to the secondary code. After calculating the circular correlation and discarding the second half of the correlation value vector, the remaining correlation values represent the correlation of the replica code with an entire code period of the original signal without any loss due to a bit transition.

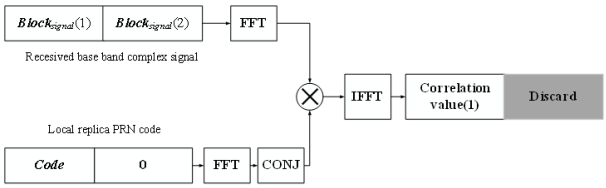

Figure 2 : Diagram of the DBZP principle.

Thanks to the efficiency of the FFT computation, the PCS and DBZP algorithms provide a high performance code search. However, in the high sensitivity context, an extended integration time is needed to obtain an additional gain. For the purpose of constraining the processing losses induced by code and carrier Doppler, more frequency search bins should be evaluated. There are two reasons for this. First, the difference of code frequency between the replica code and received code should be confined in a small value [8], otherwise, even a small code frequency misalignment would make the code phase change several chips. Second, the difference between the carrier frequency of the input signal and the local replica should be less than $1/(3T_{coh})$ [7], where T_{coh} is the coherent integration time. These limitations strongly affect the efficiency of PCS method.

The second FFT based approach of signal acquisition is the PFS approach [10]. As depicted in Figure 3. In this method, the FFT is treated as a powerful frequency spectrum analyzing tool, and this method can cover huge Doppler shift searching space, which depends on the short integrate time. The method consists of performing short coherent integration continuously, and computing the FFT on the successive correlation values. In this method, the code delay is searched sequentially while the Doppler freqeucy domain is searched in parallel by computing the FFT. If we assume that the code delay is well matched, after striping of the code modulation and calculating the short time correlation, the successive correlation value (without noise) can be expressed as [11]

$$corr(n) = \frac{(a_i d_i(t_n))sin(\pi f_D T_{coh})}{(\pi f_D T_{coh})} e^{j[2\pi f_D(t_n)+\theta_{en}]}, \quad (4)$$

where $sin(\pi f_D T_{coh})/(\pi f_D T_{coh})$ corresponds to the sensitivity loss caused by an error in the estimation of the Doppler frequency [12], t_n is the corresponding discrete time . The vector $corr(n)$ is a complex sine wave, therefore after the FFT and magnitude computation, f_D will be identified.

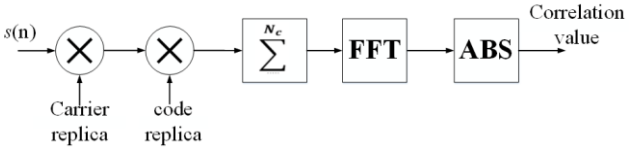

Figure 3 : Diagram of PFS algorithm.

Unfortunately, because of the increased integration time, it is difficult to use the PFS approach in high sensitivity environment. This is because several carrier frequencies are tested through the FFT while there is only one code chipping rate generated. If the code chip rate could link to the dynamic of the carrier frequency automatically, the entire frequency search space would be covered by the FFT, regardless of the total used integration time. However, the loss linked to the mismatch between the replica code chipping rate and the received code chipping rate is also affected by the dynamic of the receiver. Indeed, after long accumulation periods, the code phase will alternate. To reduce this effect, the frequency search space must be cut into several smaller bins. This will strongly affects the efficiency of PFS.

In order to reduce the acquisition time and computational burden further, the PCS and PFS can be combined together. Let us assume that the total length of the used signal is $T_{signal\_total}=(N_b+1)T_{coh}$, where N_b is the number of coherent integrations as for the requirement of the DBZP method, and the length of data should be one block bigger than the number of coherent integrations. In this design $T_{coh}=1$ ms, which corresponds to one code period or one symbol of a secondary code, and the sample rate is f_s. The carrier Doppler shift f_D is unknown and the frequency search space is $\pm f_d$ ($f_D \in [-f_d, f_d]$). As depicted in Figure 4, the original data is divided into N_b+1 blocks labeled as $\boldsymbol{block}_{signal}(1 \ldots (N_b+1))$. The code replica is generated with a certain code Doppler related to the center of the frequency search space. The total length of the generated code is one block less than the data. The code replica is divided into N_b blocks, denoted $\boldsymbol{block}_{code}(1 \ldots N_b)$.

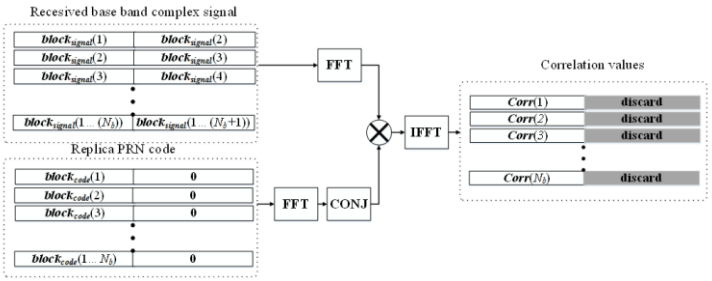

Figure 4 : DBZP-based correlation value computation.

As shown in Figure 4, the input of the data FFT module is formed by two consecutive signal blocks as [$\boldsymbol{block}_{signal}(n)$, $\boldsymbol{block}_{signal}(n+1)$], for $n \in [1, N_b]$. The input of code FFT module is formed by one code block and one block containing only zeros as [$\boldsymbol{block}_{code}(n)$,$\mathbf{0}$] where $n \in [1, N_b]$, and $\mathbf{0}$ represents a vector containing N_s zeros. Then the circular correlation of [$\boldsymbol{block}_{signal}(n)$, $\boldsymbol{block}_{signal}(n+1)$] and [$\boldsymbol{block}_{code}(n)$,$\mathbf{0}$] is computed for all n, and the second half of the correlation result is

discarded, which gives the vectors ***Corr***(n), for $n \in [1, N_b]$. Every vector contains N_s correlation values, which represent the correlation value with successive code phases. As depicted in Figure 5, the correlation matrix will be formed by merging each ***Corr***(n) column-wise. In order to simplify the expression, every cell of the matrix can be expressed as $Corr(m,n)$, where $m \in [1, N_b]$ is the row number, which represents the different code periods, and $n \in [1, N_s]$ is the column number, which represents a different code delay.

If the difference between the code replica frequency and received code frequency is small enough, every column of the matrix represents the same code delay with successive processing time. Then, by computing the FFT of the different columns separately, we will obtain the result as with the PFS search. This method, depicted in **Figure 5**, is thus similar to the PFS with $N_C = T_{coh}\, f_s$ (see figure 3) with an additional parallelism for the code delay search.

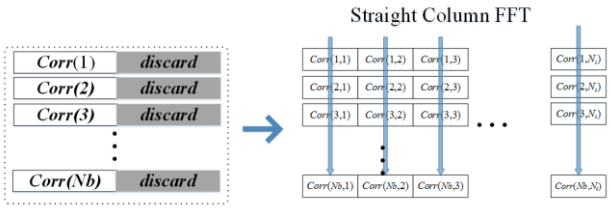

Figure 5 : Correlation value matrix structure and straight column PFS.

However, the Doppler shift search space of the PFS method depends on the code Doppler which is proportional to the chipping rate, as the code replica frequency cannot take into account different Doppler shifts, which limits the duration of the total integration time. Indeed, after a long integration time, the code Doppler induced by even a small dynamic will make the code phase change. In this case, the first correlation value and the last correlation value for every column of the correlation value matrix may correspond to different code phases. In this condition, the simple column FFT is no longer efficient, since this method cannot accumulate the correct samples together.

Considering a carrier f_L, a carrier Doppler shift f_D, and a code frequency f_{code}, the code Doppler shift can be expressed as

$$f_{D\_code} = f_{code} \frac{f_D}{f_L}. \qquad (5)$$

For the L5 signal, f_{code} is 10.23 MHz and f_L is 1176.45 MHz, therefore $f_{D\_code} = f_D / 154$. It means the received code phase shifts by one chip every $1/ f_{D\_code} = f_L/(f_D f_{code})$ second. After an integration time of t, the phase shift is thus

$$code_{phase\_shift}(t) = f_{D_{code},i}\, t = \frac{t f_D f_{code}}{f_L}. \qquad (6)$$

Let us consider a single cell of the correlation value matrix $Corr(p,q)$, and suppose that it represents the maximum of the correlation of [***block***$_{signal}$(p), ***block***$_{signal}$(p+1)] and [***block***$_{code}$(p),**0**]. After T_{coh} seconds coherent integration, due to the effect of the code chipping rate misalignment, the given correlation value of [***block***$_{signal}$(p+1), ***block***$_{signal}$(p+2)] and [***block***$_{code}$(p+1),**0**] should be $Corr(p,(q+T_{coh}f_D f_{code}/f_L))$. After m successive coherent integrations, the code phase shifting between the first row and the m^{th} row can be expressed as

$$code_{phase\_shift}(m) = \frac{T_{coh}\, f_D\, f_{code}}{f_L} m. \qquad (7)$$

According to Eq. (6) and (7), if the Doppler shift or the total integration time is small enough, then the code phase shifting value can be negligible. For example, if the T_{total} is 1 s and the Doppler span is divided in small bins of 50 Hz, then the $code_{phase\_shift}$ can be express as *50/154=0.32 chip*.

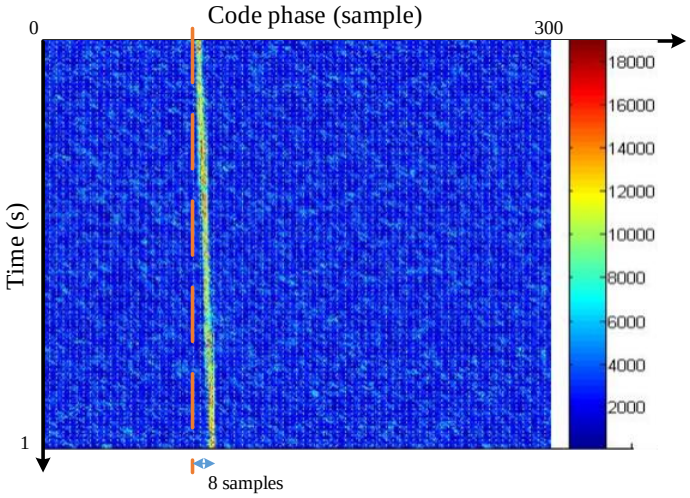

Figure 6 : Illustration of code phase shifting due to Doppler mismatch (carrier mismatch of 300 Hz here).

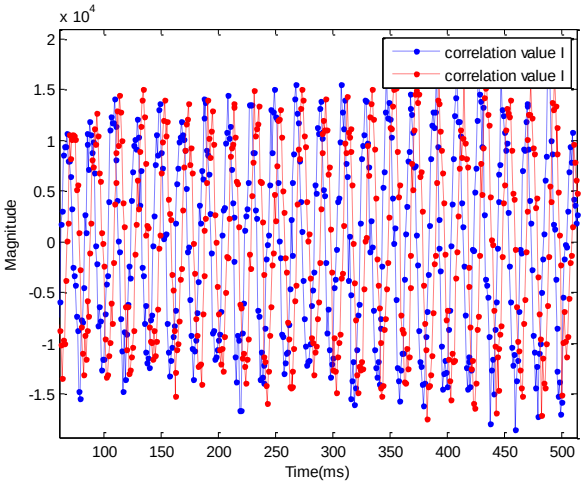

Figure 7 : Slice of the decline column with maximum magnitude of the correlation value matrix.

The phenomenon of code phase shifting is depicted in Figure 6 and Figure 7. Figure 6 represents the magnitude of the correlation value matrix ***Corr*** with a 300 Hz carrier Doppler mismatch (i.e. a mismatch of 300 / 154 ≈ 1.95 Hz code Doppler). The red dash line represents the straight column, and the high light part of this figure represents

the trace of the real code phase. It is clear that the real code phase is shifting over time; more precisely there is a shift of 8 samples in 1 s. Figure 7 shows a slice of the correlation matrix with the maximum correlation values (the highlighted part of Figure 6). In order to make this phenomenon obvious, the C/N0 used in this simulation is 45 dB-Hz and the secondary code is striped off. In high sensitivity contexts this phenomenon can be identical.

This problem increases with the total integration time, or in high Doppler shifts contexts. If the computational burden is not a concern, this problem can be solved by dividing the frequency range into smaller ranges [8] (e.g., 50 Hz), and searching every frequency range successively. In this way the code phase misalignment can be confined to a negligible level. However, since the number of carrier frequencies to search increases, the advantages of the simple PCS&PFS combined searching method will be strongly affected.

4. SLOPE PARALLEL FREQUENCY AND CODE SEARCHING (SPFCS) ALGORITHM

In order to circumvent the above described problem, we propose a new method where the code phase shifting problem is handled by a batch processing approach SPFCS algorithm. This algorithm operates both in frequency and time domain and can satisfy the requirement of long integration times. It uses DBZP to calculate the coherent integration, as in the previous algorithm, but instead of only computing the column-wise FFT in every straight column, we propose to also compute the FFT in inclined columns. For different Doppler frequency shifts, different slopes are chosen. The inclined column FFTs are illustrated in Figure 8. In this way the trace of the code phase shifting can be tracked and complemented. This method is suitable for long integration times and large Doppler shifts and the advantages of both PCS and PFS are kept.

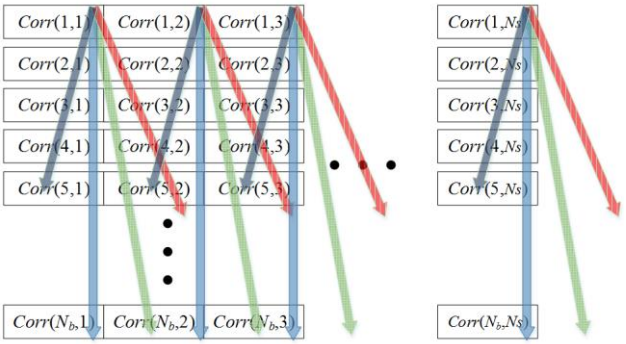

Figure 8 : Inclined column architecture.

As depicted in Figure 9, the SPFCS algorithm can be divided into 3 steps. The first step is signal preprocessing and correlation value computations, the second step is slope estimation, and the third step is inclined FFT computation and unknown secondary code complement. After these steps, the 2 dimensional (code phase & carrier Doppler shift) searching result will be obtained.

Step 1: signal preprocessing and Correlation Value Computation

In the first step, the proposed method computes the correlation of the input signal and local code through the DBZP, and stores the correlation value in a matrix, in a same way as the simple PCS&PFS combined search method described previously. After step 1 the correlation value matrix ***Corr*** is formed.

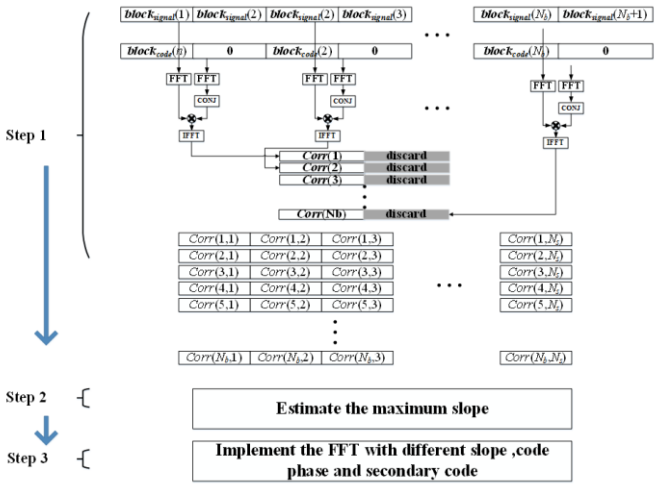

Figure 9 : Block diagram of SPFCS algorithm

Step 2: Slope Evaluation

Adapting the units of Eq. (7) to sample points by multiplying it with f_s/f_{code}, the maximum code phase shift in samples considering a maximum Doppler shift of $\pm f_d$ and a total integration time T_{total} can be expressed as

$$code_{shift\_\max\_sample} = \frac{T_{total}(\pm f_d) f_s}{f_L}. \qquad (8)$$

If the maximum code shift is less than 1 point (i.e. $code_{shift\_\max\_sample} \in [-1,1]$), a straight column wise FFT of the correlation matrix can be used, otherwise the slope column FFT should be carried out. If we assume that $Corr(1,p)$ is the correct code phase in the first row of the correlation matrix (in the pth column), the corresponding position in the last row of the matrix will be $Corr(N_b, p+code_{shift\_max\_sample})$ (in the $p+code_{shift\_max\_sample}$ column). This position will depend on the span of the carrier Doppler shift. The SPFCS algorithm can pick out all the correlation value with the same code phase and successive processing time (successive carrier phase) from the correlation matrix ***Corr*** and apply FFT computations, through inclined column wise FFT. In order to cover all the probable code phase shifts, $2code_{shift\_max\_sample}+1$ different slope values should be evaluated. Each slope value represents a different carrier Doppler shift. As depicted in Figure 10, where every black dot represents one cell of the correlation matrix, herein, the maximum code phase shift is 5 samples and therefore the number of slopes for each code phase is 11.

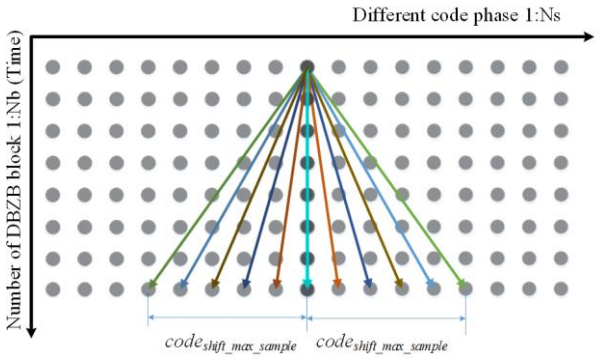

Figure 10 : Illustration of the inclined column estimation

Step 3: Inclined column FFT accumulation

The SPFCS algorithm uses a long integration time T_{toatl}, which contains N_b secondary code symbols. Since the secondary code phase of the received signal is not known for the L5 signal but its 20-bit secondary code is known, we can generate 20 different secondary code matrices from the original matrix shown in Figure 9 before computing the inclined column FFT estimations. After computing the FFT of different columns with different slopes and different secondary code phases separately, only the associated batch of correlation value with the right column number, the right secondary code combination and the right slope value will contain the maximum magnitude of these FFT computations. Herein, the column number represents the acquired code phase and the peak of the FFT output represent the acquired carrier frequency.

5. SIGNAL PROCESSING LOSS

With the proposed algorithm, there are two factors that impact the probability of detection.

The first is the loss for the received frequencies away from the replica frequency, this drawback is the same as the counterpart of the traditional PFS or PCS approach [7, 12]. It can be confined to negligible values by minimizing the searched Doppler frequency span. Supposing the frequency mismatch is confined in $1/(3T_{coh})$, the maximum of this loss will be 1.33 dB (i.e. $20\log_{10}(sinc(0.3\pi))$.

The second drawback is the extra loss called scalloping loss that occurs when the Doppler frequency falls in between two FFT bins. This loss can attain a maximum value of 3.92 dB (i.e. $20\log_{10}(sinc(\pi/2))$) if the real frequency is exactly in the middle of two FFT bins [9]. In high sensitive environment such value is unacceptable. However, it can be reduced to 0.91 dB (i.e. $20\log_{10}(sinc(\pi/4))$) by changing in the down conversion phase the local carrier frequency from f_{IF} *to* $f_{IF}+f_{bin}/2$ (where f_{bin} is the interval between two successive FFT bins), or by doubling the length of the FFT by zero-padding the input. These two methods of course increase the computational burden, but are typically required in high sensitivity context.

6. COMPUTATIONAL BURDEN ANALYSIS

The SPFCS algorithm can be implemented both in MATLAB post-processing and FPGA-based real-time processing. According to the processing flow of this particular architecture and parameters, the major computational burden is analyzed. Since the acquisition time strongly depends on the resource of the system, herein only the computational burden is analyzed.

Acquisition Architecture

We consider the acquisition architecture depicted in Figure 11. In this architecture, we included a down conversion and down sampling step [13] in order to obtain a number of samples per block that is a power of two, as we considered a FPGA implementation. Note that this step is not required for a computer or MATLAB implantation which does not require a power of two. In our example, the sampling rate f_s is 32.768 MHz.

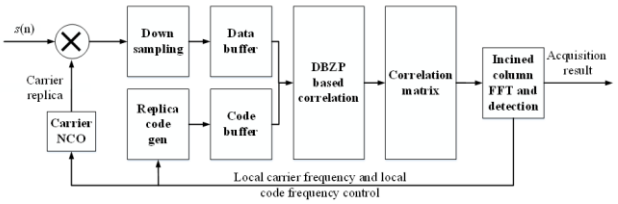

Figure 11 : Block diagram of SPFCS based acquisition module

Computational burden with SPFCS

Obviously, the major computational burden of the SPFCS algorithm comes from the FFT computations in the DBZP algorithm (i.e., step 1 in Section 4) and in the inclined column FFT computation (i.e., step 3 in Section 4). Therefore only these operations will be considered in the following analysis.

Table 1 summarizes the main parameters we will consider in our computational burden analysis.

Table 1 Major parameter clarification

Parameter	Symbol	Value
Sampling frequency	f_s	32.768 MHz
Coherent integrate time	T_{coh}	1 ms
Total integrate time	T_{total}	1 s
Frequency searching space	f_d	300 Hz
Total DBZP block number	N_b	1000
Circular correlation FFT length	N_{FFT_step1}	65536
Frequency searching FFT length	N_{FFT_step3}	1024
The maximum code shift	$Code_{shift\_max\_point}$	8.3 samples
Number of different slope	N_{slope}	18
Number of code phase in samples	$N_{codephase\_insample}$	32768

The computational burden for an FFT is assumed to be

$$Burden_{FFT}(N) = O(N \log_2 N), \quad (9)$$

Where N is the length of the FFT. Therefore the computational burden of the step 1 is

$$\begin{aligned} Burden_{SPFCS\_step1} &= Burden_{FFT}(N_{FFT\_step1}) \times 3 \times N_b \\ &= O(65536 \log_2 65536) \times 3 \times 1000 \\ &= O(3\,145\,728\,000) \end{aligned} \quad (10)$$

Since each correlation requires 2 FFTs and 1 IFFT. And the computational burden of the step 3 is

$$\begin{aligned} Burden_{SPFCS\_step3} &= Burden_{FFT}(N_{FFT\_step3}) N_{slope} \\ & N_{codephase\_in\_sample} \times 20 \\ &= O(1024 \log_2 1024) \times 32768 \times 18 \times 20 \\ &= O(67\,108\,864\,000) \end{aligned} \quad (11)$$

The factor 20 is related to the secondary code phase.

The total computational burden of SPFCS is expressed as.

$$\begin{aligned} Burden_{SPFCS} &= 2(Burden_{SPFCSstep1} + Burden_{SPFCSstep3}) \\ &= O(140\,509\,184\,000) \\ &\approx O(1.4 \times 10^{11}) \end{aligned} \quad (12)$$

The factor 2 comes from the scalloping loss control method mentioned in Section 5 (i.e., changing in the down conversion phase the local carrier frequency from f_{IF} *to* $f_{IF}+f_{bin}/2$*).*

Computational burden with DBZP and non-coherent integrations

If the traditional approach was used to accumulate these successive correlation values column wise, in order to minimize the processing loss due to the mismatch of frequency, the Doppler shift span should have been confined in a small span of [– 0.3 Hz, 0.3 Hz]. In order to cover ±300 Hz Doppler shift span that can be achieved by a single run of the SPFCS approach , the DBZP approach should be implemented 1000 times with different replica code chipping rate and local carrier frequency. So the maximum computational burden of the traditional PCS or DBZP is

$$\begin{aligned} Burden_{PCS\_maximum} &= Burden_{SPFCS\,step1} \times 1000 \\ &= O(3\,145\,728\,000\,000) \\ &\approx O(3.1 \times 10^{12}) \end{aligned} \quad (13)$$

Note that the residual of the frequency searching result does not need to be so precise, so coherent and incoherent combined integrations can be used to expend the frequency searching space and minimize the computational burden [1]. However, for the purpose of constraining the squaring loss within 1 dB, which is important in high sensitivity context, the coherent integration time should be larger than 200 ms when the C/N_0 is 18 dB-Hz or lower [14]. This means that each column accumulation in our matrix will only cover 3 Hz Doppler shift. In this case, the total computational burden of the traditional approach is

$$\begin{aligned} Burden_{PCS\_rational} &= Burden_{SPFCSstep1} \times 200 \\ &= O(6\,291\,456\,000\,000) \\ &\approx O(6.2 \times 10^{11}). \end{aligned} \quad (14)$$

This is still worse than the computational burden obtained with the proposed SPFCS approach. In addition, this method will make the residual of the acquired frequency estimation worse.

Acquisition ability comparison

Concerning all the processing losses, the acquisition ability of PCS or DBZP and SPFCS is summirized in Table 2 for a 1s total integration and 18 dB-Hz signal to noise density ratio

Table 2 : Sensitivity loss of PSC/DBZP and SPFCS assuming 1s total integration and 18 dB-Hz C/No

	PCS/DBZP	SPFCS
Code misalignment loss (dB)	1.5	1.5
Frequency mismatching loss(dB)	1.3	1.3
Scalloping loss (dB)	0	0.9
Squaring loss(dB)	1	0
Total loss(dB)	3.8	3.7

According to this Table, for a C/N0 of 18 dB-Hz and a total integration time of 1s, the PCS or DBZP approach and the SPFCS approach have the same sensitivity loss and both of these two approaches could achieve the same sensitivity. However, the computational burden of the proposed algorithm is 1/4.4 the one of the traditional PCS or DBZP method. Meanwhile, the residual of frequency searching result is 1 Hz, which is much more precise than its counterpart with the traditional method. If we consider a C/N0 of 15 dB-Hz, the computational burden of the proposed algorithm is 1/2.2 of the one of the traditional approach, and the residual of frequency searching result is 0.5 Hz.

7. SIMULATION AND RESULTS

The proposed acquisition algorithm has been tested in MATLAB simulations, for a GPS L5 signal. Some variables are modeled as uniformly distributed random variables as follows: the initial carrier phase between [$-\pi$, π] radians, the carrier Doppler shift between [-35 kHz, 35 kHz] and the initial code phase between [1, 10230]. The other used parameters are the ones mentioned in Section 6.Figure 12, Figure 13 and Figure 14 show the acquisition result of the proposed algorithm for different high sensitivity contexts.

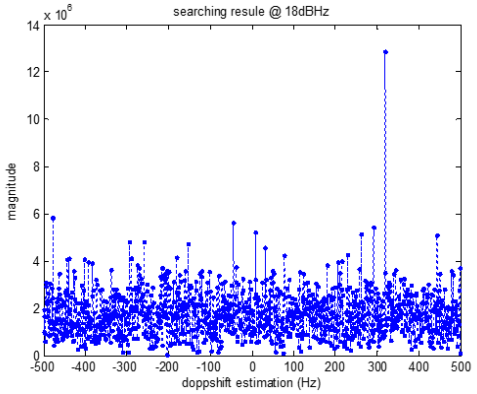

Figure 12 : Acquisition result with a C/N0 of 18 dB-Hz and T_{total} of 1 s.

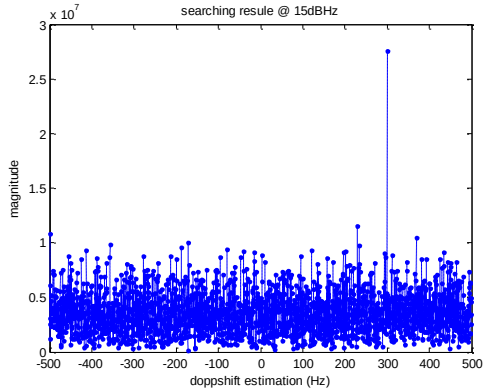

Figure 13 : Acquisition result with a C/N0 of 15 dB-Hz and T_{total} of 2 s.

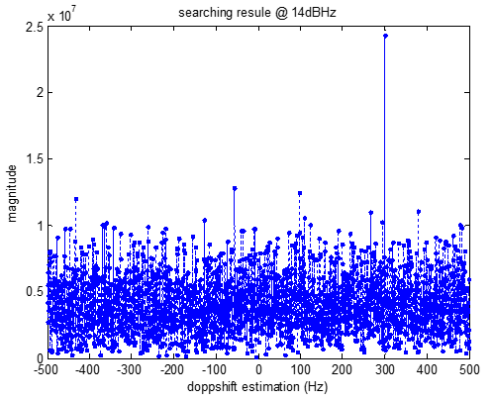

Figure 14 : Acquisition result with a C/N0 of 14 dB-Hz and T_{total} of 2 s.

The maximum Doppler estimation error is 1 Hz with 1 s integration and 0.5 Hz with 2 s integration, and both the code phase and secondary code combination are well matched.

To further assess the performance of the SPFCS algorithm, Monte Carlo simulations have been performed. The results indicate that the proposed algorithm can successfully acquire signal as low as 15 dB-Hz in 35 kHz Doppler shift environment with 2 seconds total integration time. According to the different sensitivity requirements, different T_{total} should be chosen. The performance of this algorithm in different contexts is summarized in **Table 3**.

Table 3 Alarm rate of SPFCS algorithm in different context

C/N_0 (dB-Hz)	Number of experiments	Detection times	False alarm times	Remark
14	100	80	0	T_{total}=2 s
15	100	95	0	T_{total}=2 s
18	100	93	0	T_{total}=1 s

Remark: The acquisition threshold used in the simulation was selected empirically and has not been optimized.

8. SUMMARY AND CONCLUSIONS

The proposed SPFCS algorithm combines the PCS and PFS together. This algorithm can achieve the high sensitivity requirement by solving the problem of code phase shifting and taking advantage of both the PCS and PFS methods. The proposed algorithm has three major advantages. Firstly, by solving the problem of code phase shifting, long coherent integration times can be achieved without the limitation of Doppler shifts and squaring losses. Secondly, compared to the traditional PCS or DBZP algorithm, the computational burden is reduced significantly. Finally, the Doppler shift estimated is much more accurate than the one of the PCS approach.

The Simulation results have shown that without any assistance, the proposed algorithm can acquire a signal as weak as 15 dB-Hz with 2 s total coherent integration or 18 dB-Hz with 1 s total coherent integration.

ACKNOWLEDGMENTS

The author would like to thank EPFL and CAST Xi'an for their financial supports for this research.

REFERENCES

[1] J. Leclère, C. Botteron and P.-A. Farine. Acquisition of modern GNSS signals using a modified parallel code-phase search architecture, in Signal Processing, vol. 95, p. 177-191, 2014.

[2] J. Leclère, C. Botteron, P-A. Farine, "Comparison Framework of FPGA-based GNSS Signals Acquisition Architectures", IEEE Transactions on Aerospace and Electronic Systems, Vol. 49, No. 3, pp. 1497-1518, (2013).

[3] J.B.-Y. Tsui, "Fundamentals of Global Positioning System Receivers: A Software Approach", John Wiley & Sons Inc, 2nd Edition, 2005.

[4] D. Akopian, "Fast FFT based GPS satellite acquisition method", IEE Proceedings - Radar, Sonar and Navigation, vol. 152, no. 4, pp. 277–286, Aug. 2005.

[5] M Foucras, O. Juliena, Christophe Macabiau, Bertrand Ekambi "Novel Computationally Efficient Galileo E1 OSAcquisition Method for GNSS Software Receiver" ION GNSS 2012, Sept. 2006.

[6] IS-GPS-705C, "Navstar GPS Space Segment/User Segment L5 Interfaces", Jan 2013.

[7] E. Kaplan, C. Hegarty, "Understanding GPS: Principles and Applications", Artech House, 2nd Edition, 2005.

[8] N.I. Ziedan, J. L. Garrison, "Unaided Acquisition of Weak GPS Signals Using Circular Correlation or Double-Block Zero Padding", Proc. of the IEEE Position Location and Navigation Symposium (PLANS), 2004.

[9] D. M. Lin, J.B.Y. Tsui and D. Howell, "Direct P(Y)-Code Acquisition Algorithm for Software GPS Receivers" in Proc. ION GPS-99, 1999.

[10] S.M. Spangenberg, G.J.R. Povey,"Code acquisition for LEO satellite mobile communication using a serial-parallel correlator with FFT for Doppler estimation", Proceedings of First International

Symposium on Communication Systems and Digital Signal Processing, 1998, Proceedings of IST

[11] J.A. Del Peral-Rosado, "Kalman Filter-Based Architecture for Robust and High-Sensitivity Tracking in GNSS Receivers", Satellite Navigation Technologies and European Workshop on GNSS Signals and Signal Processing (NAVITEC), 5th ESA Workshop, 2010.

[12] C. Botteron, G. Walchli, G. Zamuner, M. Frei, D. Manetti, F. Chastellain, P-A. Farine, P. Brault, "A Flexible Galileo L1 Receiver Platform for the Validation of Low Power and Rapid Acquisition Schemes", ION GNSS 2006, Forth Worth, Texas, USA, Sept. 2006.

[13] J.A. Starzyk, Z. Zhu, "Averaging correlation for C/A code acquisition and tracking in frequency domain", IEEE 2001 Midwest Symposium on Circuits and Systems, Dayton, Ohio, USA, Aug. 2001.

[14] C. Strässle, D. Megnet, H. Mathis, "The Squaring-Loss Paradox" ION GNSS 20th International Technical Meeting of Satellite Decision September 2007, Fort Worth, TX.